

Catalysts Based on Fiberglass Supports: II. Physicochemical Properties of Alumina Borosilicate Fiberglass Supports

L. G. Simonova*, V. V. Barelko**, E. A. Paukshtis*, O. B. Lapina*,
V. V. Terskikh*, V. I. Zaikovskii*, and B. S. Bal'zhinimaev*

* Boreskov Institute of Catalysis, Siberian Division, Russian Academy of Sciences, Novosibirsk, 630090 Russia

** Institute of Problems of Chemical Physics, Russian Academy of Sciences, Chernogolovka, Moscow oblast, 142432 Russia

Received March 13, 2000

Abstract—The properties of borosilicate fiberglass supports were studied using a set of physicochemical techniques (BET; transmission electron microscopy; IR spectroscopy; and ^{11}B , ^{23}Na , ^{27}Al , and ^{29}Si NMR spectroscopy). Unleached fiberglass was characterized by the presence of silicon primarily in the Q^2 form (two silicon atoms in the second coordination sphere of silicon–oxygen tetrahedrons) and by a comparatively homogeneous distribution of concomitant heteroatoms (B, Al, and Na). Under the action of an acid, the extraction of nonsilica components and the rearrangement of a silicon–oxygen framework (the transition of Q^2 to $Q^3 + Q^4$) took place simultaneously. This was accompanied by the development of the surface and by the formation of channels with a wide range of sizes: from channels 15–50 Å in diameter (the adsorption properties of these channels are similar to those of mesopores in ordinary silica supports) to microchannels, which are typical of pseudolayer intercalation structures described previously for leached soda–silica fiberglass.

INTRODUCTION

Porous borosilicate glasses are in large-scale commercial production both in Russia and abroad. Because the porous structure can be widely controlled and products of various geometric shapes can be made, porous glasses are extensively used in chromatography and laser engineering, as well as for preparing semipermeable membranes, molecular sieves, etc. [1]. The use of powdered or pelletized porous glasses as catalyst supports is well known. In a number of cases, this improved the catalytic activity of supported phases [2]. The use of fiberglass supports offers additional advantages [3–6]. The physicochemical properties of leached fiberglass systems are not clearly understood, particularly from the standpoint of their applicability as catalyst supports. Previously [7], we considered the properties of fibrous silica materials prepared from homogeneous soda–silica glasses. Borosilicate glasses can exhibit heterogeneity because of their ability to undergo phase separation on cooling a molten glass below a liquidus. This can affect the texture characteristics of porous materials prepared by leaching these glasses [1].

In this work, we studied the physicochemical properties of porous materials prepared by leaching alumina borosilicate fiberglass materials.

EXPERIMENTAL

Commercial fiberglass of alumina borosilicate E-Glass was selected, containing 53% SiO_2 , 15% Al_2O_3 ,

10% B_2O_3 , 15% CaO , 0.5% Na_2O , and the balance $\text{MgO} + \text{TiO}_2 + \text{Fe}_2\text{O}_3$. A sizing agent used in the industrial production of glass fiber was removed by calcination at 650°C or washing with a 5% ammonia solution. The leaching was performed with the use of a 5.5% HNO_3 solution; the temperature and duration were varied from 20 to 90°C and from 10 to 60 min, respectively.

The samples were designated by numbers corresponding to the temperature and duration of leaching (for example, EB-20-10 is a sample leached at 20°C for 10 min).

The Si, Al, B, Mg, Ca, and Na contents were determined by atomic absorption spectrometry. The specific surface areas were determined by BET using the thermal desorption of argon (S^{Ar}) and by titration with a solution of NaOH (S^{Na}) [7, 8].

The morphology of samples was studied by transmission electron microscopy (TEM) on JEM-100CX and JEM-2010 electron microscopes.

The structure of initial and leached materials was studied by ^{29}Si , ^{27}Al , ^{23}Na , and ^{11}B MAS NMR spectroscopy. The MAS NMR spectra were measured on a Bruker MSL-400 pulse Fourier transform NMR spectrometer (magnetic field of 9.4 T) under conditions specified in Table 1. The magic-angle spinning (MAS) of samples was performed using a high-speed probe (NMR Rotor Consult ApS, Denmark) with silicon nitride and zirconia rotors (5 mm o.d.) at a rate of 8000–10000 Hz.

The properties of SiOH groups were examined by the IR spectroscopy of adsorbed molecules using an

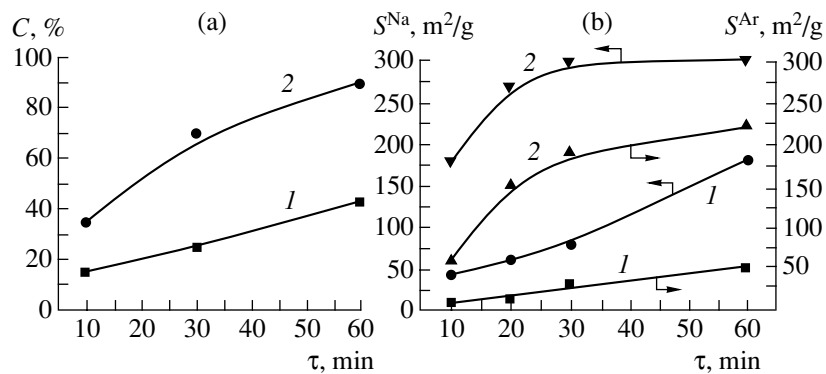


Fig. 1. Effects of the time (τ) and temperature ($T = (1) 20$ and (2) 90°C) of acid treatment of borosilicate fiberglass on (a) the degree of leaching of nonsilica components ($C, \%$) on a boron basis and (b) the specific surface areas (S^{Ar} and S^{Na}).

IFS-113v spectrometer (Bruker) in the range 1100 – 7000 cm^{-1} with a resolution of 4 cm^{-1} . All of the spectra were analyzed by deconvoluting absorption band profiles into individual Gaussian components using the ORIGIN 5.1 software. The sample preparation procedures, the measurement of spectra, and the calculation of OH group concentrations were detailed previously [7].

RESULTS

Chemical Composition and Texture of Leached Fiberglass

The specific surface area of unleached fiberglass is low ($\sim 1\text{ m}^2/\text{g}$). After an acid treatment, the concentrations of nonsilica components decreased, and this decrease depended on the temperature and duration of the treatment. Figure 1a demonstrates the effects of temperature and duration of the acid treatment on the degree of leaching (C), as evaluated by the degree of boron removal from the samples. The extraction of nonsilica components was accompanied by an increase in the specific surface area. Thus, as the leaching time increased from 10 to 60 min, the values of 20°C S^{Ar} increased from 10 to 50 or from 60 to $220\text{ m}^2/\text{g}$ at a temperature of 20 or 90°C , respectively (Fig. 1b). It is important to note that in all cases, S^{Na} was higher than

S^{Ar} . Hence, it is likely that very small microcavities, which are accessible only to sodium cations, were also formed in the system along with pores accessible to argon. Note that, in contrast to borosilicate fiberglass, only such microcavities were formed on leaching soda–silica fiberglass [7].

The surface area changed on the calcination of leached fiberglass, and this change strongly depended on temperature and on the degree of leaching. In samples with a high degree of leaching (75–90%), the specific surface area changed only slightly on calcination at 500°C , and a detectable change in this value occurred at higher temperatures. At degrees of leaching lower than 50%, the thermal stability of fiberglass was low, and a decrease in the specific surface area by a factor of 7–10 was observed at 550°C . It is likely that the presence of impurity cations (B, Ca, and Na) is favorable for sintering, as is the case with many silica systems [8].

It is well known that, in the production of conventional Vycor porous glasses starting from powdered or pelletized borosilicate glasses, the degree of leaching of concomitant cations approaches 100%, and a skeleton of almost pure SiO_2 is formed. An important feature of fibrous borosilicate glasses is a decrease in the mechanical strength as the degree of leaching increases. The loss of strength increases in samples subjected to high-temperature calcination both before and after leaching. Strength appropriate for the subsequent use of fiber-

Table 1. Conditions of measuring MAS NMR spectra

Nucleus	Nuclear spin	Resonance frequency, MHz	Scan frequency, kHz	Pulse duration, μs	Interpulse delay, s	Scan number	Reference
^{11}B	3/2	128.38	30	1	0.5	2048	H_3BO_3 1M
^{23}Na	3/2	105.81	25	2	0.1	450	NaCl 0.1M
^{27}Al	5/2	104.23	100	2	1	300	$\text{Al}(\text{NO}_3)_3$ 1M
^{29}Si	1/2	79.49	30	4	20	300–2000	TMS*

* TMS is tetramethoxysilane.

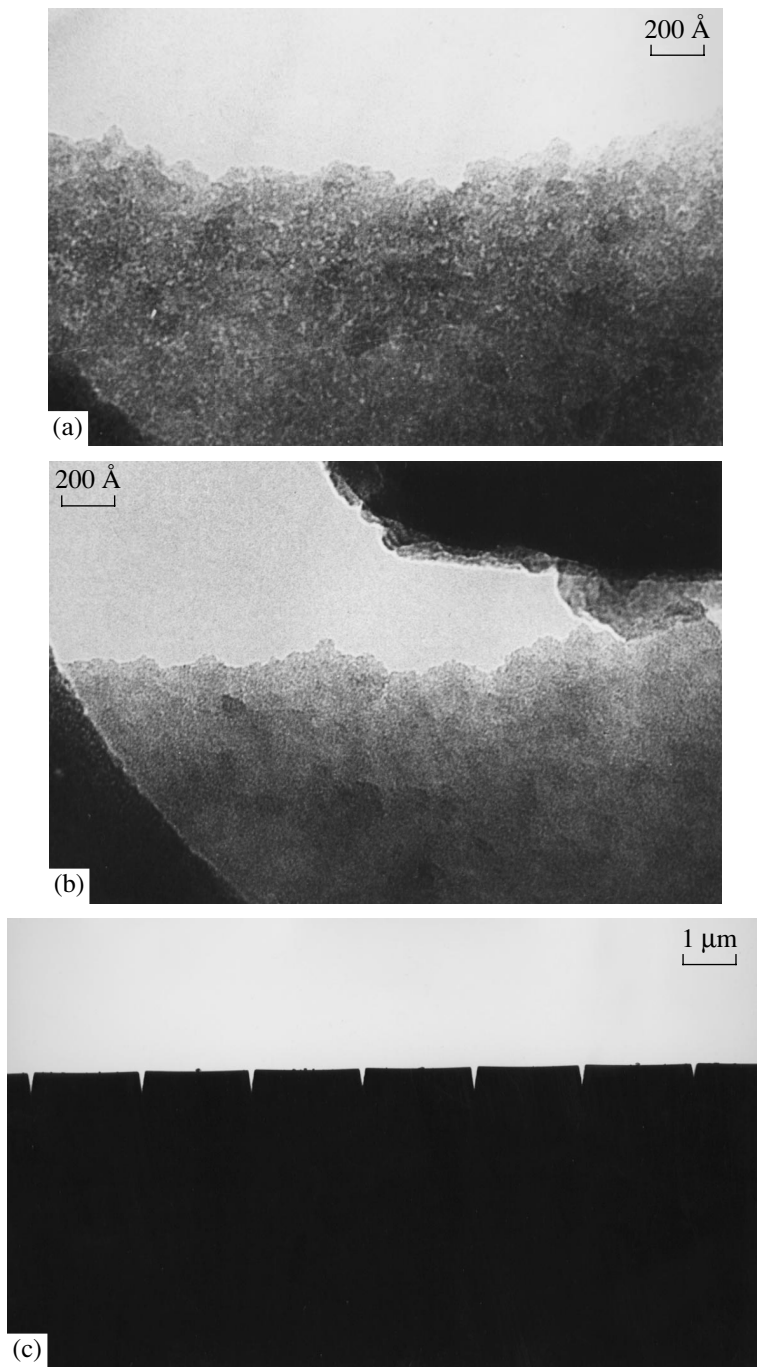


Fig. 2. TEM micrographs of leached fiberglass: (a) sample EB-20-60, the degree of leaching $C \sim 35\%$; (b) sample EB-90-60, $C \sim 85\%$; and (c) wedge-shaped cracks on the outer surface of sample EB-90-30, $C \sim 70\%$.

glass products can be retained at degrees of leaching $<50\%$. After this partial leaching, the fiber core, which is responsible for the mechanical properties of the material, almost completely retained its initial physical and chemical state, whereas leachable constituents were removed from surface layers as fully as possible. In this work, we considered samples with both low and high degrees of leaching.

Morphology According to Electron-Microscopic Data

The internal structure of fibers depends on the degree of leaching of nonsilica constituents. In sample EB-20-60 with a comparatively low degree of leaching ($\sim 35\%$), sponge surface zones were formed on the outer surface. These zones manifest themselves in electron micrographs as light spots wormlike in shape; they can be ascribed to mesopores 15–50 Å in diameter and up

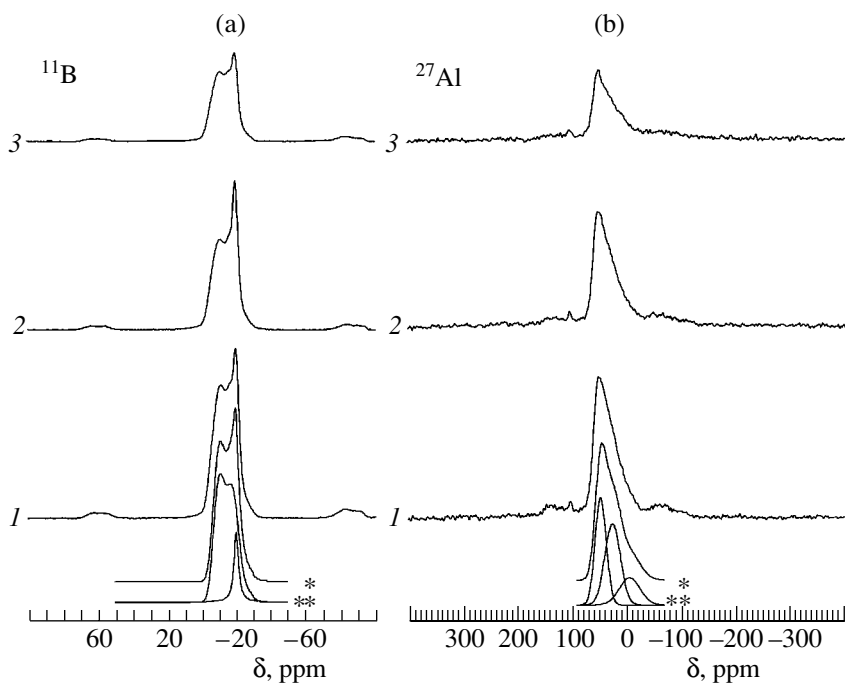


Fig. 3. (a) ^{11}B and (b) ^{27}Al MAS NMR spectra of borosilicate fiberglass: (1) unleached sample E-0; (2) sample EB-20-10, the degree of leaching $C \sim 18\%$; and (3) sample EB-20-60, $C \sim 35\%$. * Simulated spectrum. ** Components of the simulated spectrum.

to 200 Å long (Fig. 2a). The above difference between S^{Na} and S^{Ar} is indicative of the presence of micropores in leached fiberglass. These micropores are difficult to observe using TEM. However, as in soda–silica systems [7], a structural transformation under exposure to an electron beam is indirect evidence of the presence of micropores. In this case, the displacement of microheterogeneous regions and increase in their size can be explained by the sintering of micropores.

An increase in the degree of leaching initially resulted in an increase in the number and size of pores; then, the internal structure underwent a considerable rearrangement. Thus, in a sample with a degree of leaching $>50\%$, pronounced wormlike pores were not observed; the structure became loosened, and the micrographs exhibited a grainy background with a grain size of ~ 20 Å. At degrees of leaching $>70\%$, the samples underwent considerable structural transformations with the rearrangement of individual grains and the formation of dense regions (Fig. 2b). Simultaneously, the pore size increased because of the coalescence of neighboring pores. As shown in Fig. 2c, large wedge-shaped cracks up to 1000–2000 Å wide and up to 5000 Å deep appeared on the outer surface of fibers. As the degree of leaching increased, the cracks grew and the fibers lost their strength and underwent degradation.

Properties of Borosilicate Fiberglass According to NMR Data

In the NMR studies of fiberglass, primary attention was focused on the following two aspects: (1) the effect of leaching on the amount and state of acid-soluble constituents of the fiberglass (B, Al, and Na) and (2) the structure of the residual silicon–oxygen framework.

^{11}B NMR spectra. ^{11}B MAS NMR spectroscopy is one of the most informative physicochemical techniques for studying the state of boron in boron-containing materials such as borosilicates and borates [9, 10]. The ^{11}B nucleus has the nuclear spin $I = 3/2$ and a quadrupole moment of $0.04 \times 10^{-24} \text{ cm}^2$.

In chemical compounds, boron may exhibit a tetrahedral (BO_4) or trigonal (BO_3) environment. In this case, as measured by NMR spectroscopy, the quadrupole coupling constant is as high as 4 MHz for the trigonal environment, whereas it is much lower (200–500 kHz) for the tetrahedral environment. Consequently, the trigonal coordination and tetrahedral coordination of boron are easy to distinguish by NMR spectra: the line corre-

Table 2. Relative integrated intensities of signals from various nuclei in the NMR spectra of borosilicate fiberglass

Sample	^{11}B	^{23}Na	^{27}Al	$^{29}\text{Si}(Q^2)$
E-0	100	100	100	100
EB-20-10	82	82	81	70
EB-20-60	59	71	67	62

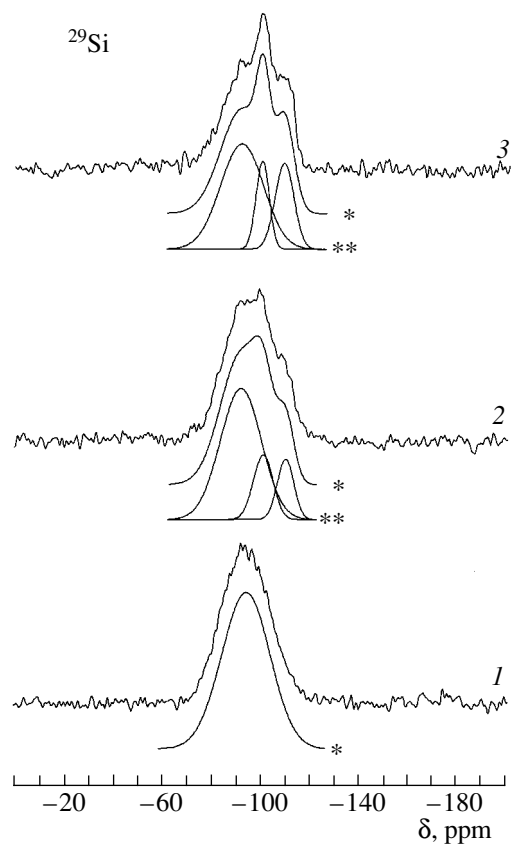


Fig. 4. ^{29}Si MAS NMR spectra of borosilicate fiberglass: (1) sample E-0; (2) sample EB-20-10, the degree of leaching $C \sim 18\%$; and (3) sample EB-20-60, $C \sim 35\%$. * Simulated spectrum. ** Components of the simulated spectrum.

sponding to the tetrahedral boron is narrow, whereas the line due to trigonal boron has the shape of a doublet, which is typical of quadrupole splitting. The range of ^{11}B chemical shifts is narrow; therefore, the lines due to boron in trigonal and tetrahedral coordination may overlap.

The ^{11}B MAS NMR spectrum of unleached fiberglass (sample E-0) is a superposition of two lines (Fig. 3, spectrum 1), which correspond to boron in tetrahedral (7%) and trigonal (93%) coordination. For the latter, the line has the shape of a characteristic doublet

Table 3. Relative integrated intensities of components in the ^{29}Si MAS NMR spectra of borosilicate fiberglass

Sample	Q^2 ($\delta = -95$ ppm)	Q^3 ($\delta = -100$ ppm)	Q^4 ($\delta = -110$ ppm)
E-0	100	—	—
EB-20-10	70	17	13
EB-20-60	62	16	22

(Fig. 3, spectra 2, 3), which is typical of boron in the trigonal environment BO_3 with the quadrupole coupling constant $C_Q = 2.6$ MHz, the asymmetry parameter $\eta = 0.3$, and an isotropic shift of -4 ppm. Similar spectral parameters were observed for the planar trigonal coordination of boron in borates and oxides [10, 11].

Leaching at 20°C for 10 min resulted in a decrease in the boron content of the sample by 18% (Fig. 1a); this is consistent with chemical analysis data (Table 2). In this case, the state of boron that had not passed into solution was similar to that in the initial sample: 89 and 11% of total boron were present in trigonal and octahedral coordination, respectively.

Leaching at 20°C for 60 min resulted in an even higher extraction of boron from the sample. The ^{11}B NMR spectrum indicated a decrease in the boron content by 41% with respect to the parent material (Table 2); this value is close to the degree of leaching determined by chemical analysis ($\sim 35\%$). The coordination state of boron was the same as in the parent material: 92 and 8% of total boron were present in trigonal and octahedral coordination, respectively (Fig. 3, spectrum 3).

^{23}Na NMR spectra. The ^{23}Na MAS NMR spectra of initial samples and samples leached at 20°C for 10 and 60 min exhibited a very broad asymmetric unstructured low-intensity line with a maximum at about -25 ppm. That is, the local environment of sodium was significantly distorted, and it cannot be represented as a superposition of discrete states. This can be explained by the irregular coordination environment of sodium in multi-component borosilicate glass. The relative integrated intensity of the spectrum, which corresponds to the relative sodium content of the sample, decreased on going from unleached sample E-0 to samples EB-20-10 and EB-20-60 (Table 2). It is important that the structure (shape) of the ^{23}Na MAS NMR spectrum remained almost unchanged in the course of leaching.

^{27}Al NMR spectra. The ^{27}Al MAS NMR spectra of the test samples of borosilicate fiberglass before and after leaching with nitric acid are shown in Fig. 3. The spectra of initial sample E-0 and samples after leaching are similar in shape: an asymmetric line, which is a superposition of three Gaussian shape lines (spectra 1–3). A narrower line with a chemical shift of 53 ppm can be attributed to aluminum in a tetrahedral oxygen environment, whereas broader lines with chemical shifts of about 31 and 2 ppm should be assigned to aluminum in pentahedral and octahedral oxygen coordination, respectively. Although the total aluminum content decreased in the course of leaching (81 and 67% in samples EB-20-10 and EB-20-60, respectively), the relative concentrations of different structural states of aluminum in the samples remained almost unchanged.

^{29}Si NMR spectra. The ^{29}Si MAS NMR spectra of the test samples and the results of their deconvolution into Gaussian components are presented in Fig. 4 (spectra 1–3) and Table 3. The spectrum of the initial

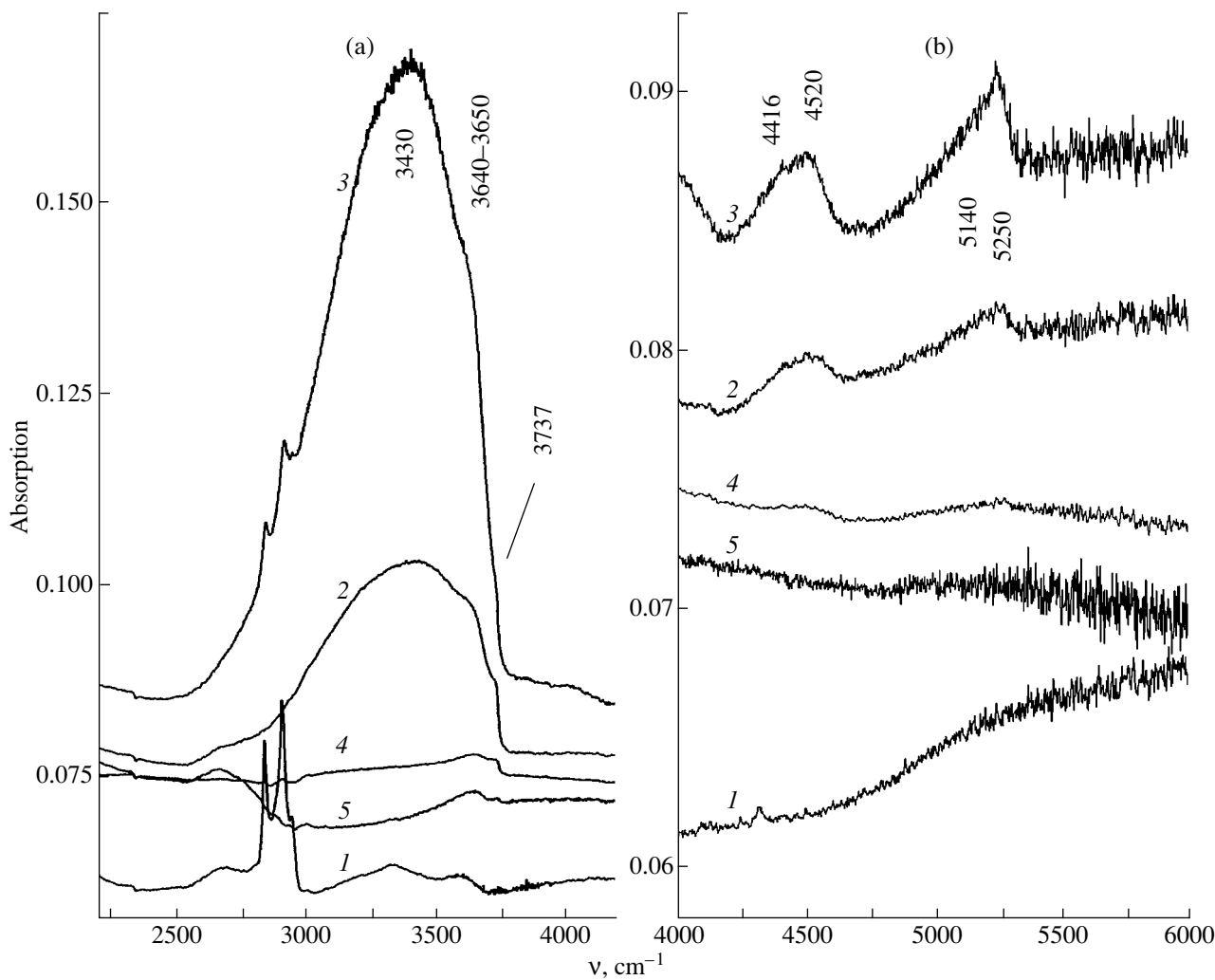


Fig. 5. IR spectra of borosilicate fiberglass in the (a) stretching and (b) combination regions: (1) unleached sample E-0; (2) sample EB-90-10, $C \sim 35\%$, drying temperature of 110°C ; (3) sample EB-90-60, $C \sim 85\%$, 110°C ; (4) sample EB-90-10, 550°C ; and (5) sample EB-90-10, 900°C . The absorption on an absorbance scale is reduced to the weight of 1 cm^2 sample (mg/cm^2). The specified frequencies were obtained by deconvoluting the spectra.

sample consists of a single broadened Gaussian line with a chemical shift of -94 ppm . Judging from the chemical shift, this line can be assigned to Q^2 groups, when two silicon atoms are present in the silicon–oxygen tetrahedrons in the second coordination sphere, and the other two positions are occupied by heteroatoms [7, 9, 12]. This state of silicon predominated in initial sample E-0.

After leaching a sample for 10 min, its spectrum dramatically changed and became a superposition of three lines. A higher intensity line (70%) with a chemical shift of -95 ppm has the same nature as that in the initial sample; that is, it can be attributed to groups of the Q^2 structural type. The line with a characteristic chemical shift of -100 ppm is assigned to groups of the Q^3 type—three silicon atoms in the second coordination sphere of silicon–oxygen tetrahedrons [9, 12]. The relative amount of these groups was 17% of the total

amount of silicon in the sample. The lower intensity upfield line with a chemical shift of -110 ppm is assigned to the Q^4 structural groups (13% of total silicon in the sample).

Long-term leaching (sample EB-20-60) resulted in even more pronounced changes in the ^{29}Si MAS NMR spectrum (Fig. 4, spectrum 3). In this case, the concentration of Q^4 groups (22%, a line with a chemical shift of -110 ppm) increased because of a decrease in the amount of Q^2 units (62%, a line with a chemical shift of -95 ppm) at an almost unchanged concentration of Q^3 groups ($\sim 17\%$, a line with a chemical shift of -100 ppm).

Thus, according to NMR data, the initial sample consists of a homogeneous glass with a disordered arrangement of both anionic and cationic structural units. The silicon–oxygen tetrahedrons are primarily in

Table 4. Stretching and bending vibrational frequencies, as measured experimentally and calculated from the frequencies of mixed vibrational modes

Sample	v, cm^{-1}				
	SiO stretching	Si—O—H bending	OH stretching		combination
			SiOH groups	H_2O molecules	
SiO_2 500°C, vacuum	770	870	3740	—	—
CB (110°C)*	770	870	3640	—	4410, 4510
	—	—	—	3610	5240
EB-20-60, dried at 110°C	—	—	3737	—	—
	780	880	3640	—	4420, 4520
	—	—	—	3510	5140
	—	—	—	3620	5250

* According to data [7].

the Q^2 state; apart from two silicon atoms, they bear two heteroatoms (B, Na, or Al) each in the second coordination sphere. Boron primarily (93%) occurs in trigonal coordination with oxygen atoms, which is typical of boron-containing glasses [10]. It is likely that aluminum and sodium are characterized by a wide distribution of possible states, which is also typical of vitreous samples [9].

The treatment of samples with a nitric acid solution resulted in the extraction of acid-soluble compounds of boron, sodium, aluminum, etc. The concentrations of these elements proportionally decreased as the duration of leaching increased. Although each of the leached components occurred as several structural forms in the sample, the preferential extraction of any of these species was not observed in the course of acid treatment. This may be indicative of the uniformity (homogeneity) of the distribution of dissolved components throughout the glass volume, as well as of the same resistance of various coordination species to acid dissolution.¹

The remaining silicon–oxygen framework underwent structural transformations. In unleached glass, all silicon occurs in the Q^2 form. This fact is indicative of an almost complete absence of extended regions of silicon–oxygen tetrahedrons, which are characterized by a large fraction of silicon in the Q^4 form. That is, it is reasonable to suggest a uniform distribution of Si in the volume of other constituents of unleached glass (boron, aluminum, etc.). It is important that after leaching the fractions of Q^2 and acid-soluble components decreased in approximately the same proportion (~40% for sample EB-20-60); however, $Q^3 + Q^4$ simultaneously

appeared in the same amount (Table 3). Thus, in the course of leaching, a portion of silicon attained the Q^3 (with one heteroatom in the second coordination sphere) and Q^4 (all silicon atoms in the second coordination sphere) coordination. These states of silicon are typical of ordinary silica [9, 12] and leached soda–silica glasses described previously [7].

State of OH Groups in B–Si Fiberglass According to IR-Spectroscopic Data

Figure 5a demonstrates the spectra of OH groups in borosilicate fiberglass samples which were leached and calcined under different conditions. The spectra of initial sample E-0 are characterized by absorption bands at 3600 and 3350 cm^{-1} , which were assigned to residual OH groups. Three intense bands at 2850–2950 cm^{-1} were attributed to unremovable residues of organic oils, which are used in fiberglass manufacture. In the course of leaching, three bands at 3430, 3640–3650, and 3737 cm^{-1} appeared and increased in intensity (Fig. 5a, spectra 2, 3). The first of these bands was assigned to OH groups bound with strong hydrogen bonds, and the second band of OH groups is analogous to that detected previously in silica fiberglass [7]. The third band was attributed to free SiOH groups, which are analogous to those observed in silica gels with highly developed surfaces [8, 13, 14]. For sample EB-90-10 (degree of leaching of ~30%; dried at 110°C), we calculated the concentrations of OH groups of these types to be 830, 320, and 170 $\mu\text{mol/g}$, respectively, which add up to 1320 $\mu\text{mol/g}$. In sample EB-90-60, in which the degree of leaching was as high as ~85%, the amount of OH groups increased by a factor of 2 to 3 and approximated 3500–4000 $\mu\text{mol/g}$.

In the region of combination modes (Fig. 5b), absorption bands were detected whose positions were somewhat different from the band positions in soda–silica glasses. Bands at ~4416 and 4520 cm^{-1} were

¹ We found in special experiments that the absence of pronounced selectivity of leaching is a common feature of the fibrous borosilicate test materials, which was exhibited by all matrix components (i.e., not only B and Al but also Ca and Mg). However, the kinetics of leaching is a problem of fundamental importance and should be studied additionally.

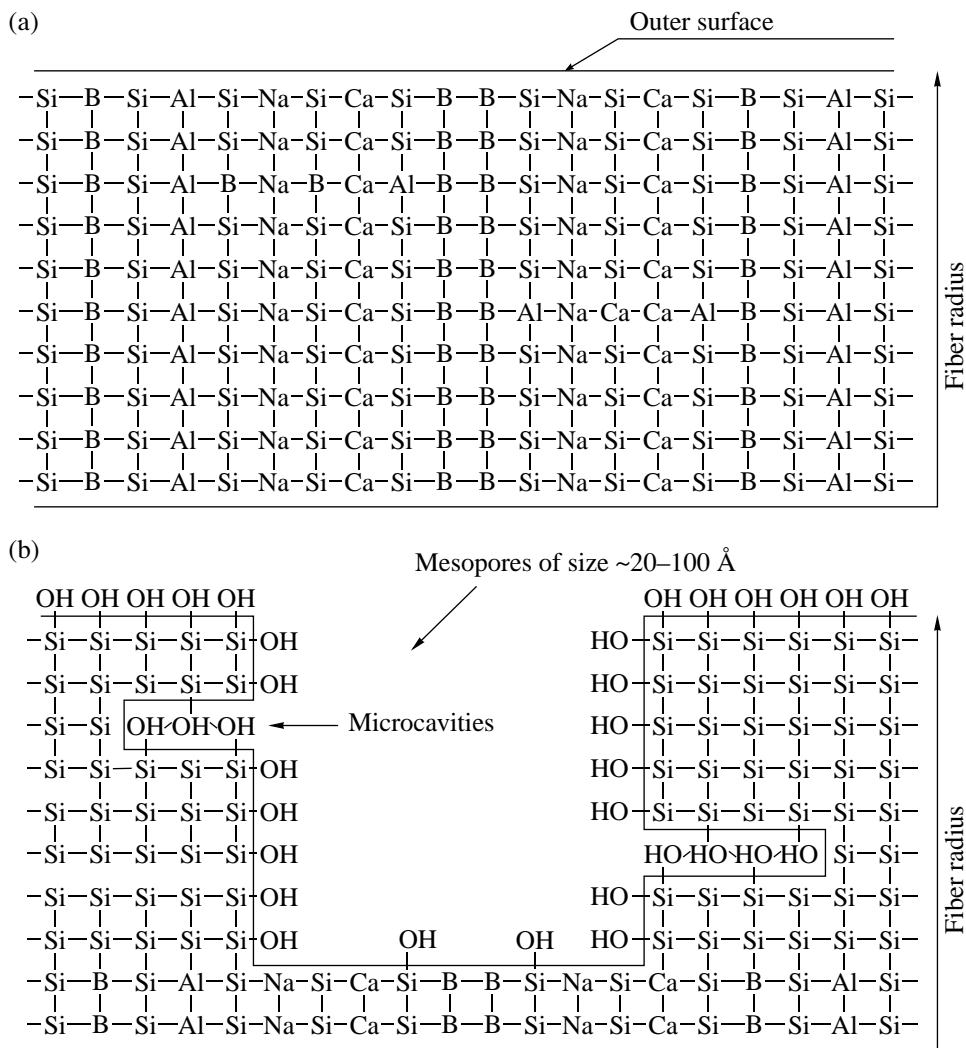


Fig. 6. Schematic diagram of texture transformations on leaching borosilicate fiberglass: (a) starting fiberglass and (b) fiberglass after the extraction of heteroatoms and a rearrangement of the remaining silicon–oxygen units.

observed for SiOH vibrations, and bands at 5140 and 5250 cm^{-1} were detected for water vibrations.

Table 4 summarizes the values calculated for SiOH bending vibrations and OH stretching vibrations in water molecules. By comparison with the data on silica fiberglass [7], we found that borosilicate fiberglass exhibited two types of molecular water and two types of SiOH groups. One of these types of OH groups and one type of molecular water are similar to those detected in silica fiberglass, whereas the other are more similar to those in ordinary silica gels [8, 13, 14].

Thus, according to IR-spectroscopic data, porous spaces of two types can be recognized in leached borosilicate glasses. One of these types is characterized by weak hydrogen bonds (the vibrational bands of OH and molecular water at 3640 and 3620 cm^{-1} , respectively), and the other type (bands at 3737 and 3510 cm^{-1}) is similar to mesopores in ordinary silica gels.

The total number of OH groups decreased on the calcination of borosilicate samples; however, the bands at 3640 and 3737 cm^{-1} were retained even at 900°C, although the band intensities were lower. The spectra of a sample calcined at 900°C exhibit a band at 2600–2700 cm^{-1} , which can be assigned to SiO stretching vibrational overtones.

DISCUSSION

We experimentally found that leached borosilicate fibers differ from the previously described silica fiberglass supports [7] in a number of properties.

According to the data obtained by electron microscopy and by the measurement of specific surface area, pores from several angstroms to 50 Å in diameter and up to 200 Å in length were formed in borosilicate fiberglass at medium degrees of leaching (up to 50%). These pores propagated from the outer surface to the core of

fibers. The wide range of pore sizes was confirmed by IR spectroscopy. These data suggested the presence of terminal SiOH groups (3737 cm^{-1}), which usually occur at the surface of silica mesopores, and specific SiOH groups (3640 cm^{-1}), which are typical of microcavities in the pseudolayer structures of leached Na–Si fiberglass [7], although, in smaller amounts. Molecular water (combination band at $\sim 5240\text{ cm}^{-1}$) was also detected.

The formation of such structures on leaching can be described by the model schematically depicted in Fig. 6. According to NMR data, unleached borosilicate fiberglass is characterized by the presence of silicon predominantly in the Q^2 form with a comparatively homogeneous distribution of heteroatoms (Fig. 6a). Under the action of an acid, concomitant cations are simultaneously extracted in proportional fractions and the silicon–oxygen framework is rearranged (the transition of Q^2 to $Q^3 + Q^4$). It is believed that etched channels are formed after the extraction of soluble components, and the remaining adjacent Q^2 silicon units are very unstable; therefore, they are readily joined by the cross-linking of neighboring layers. The adjacent cavities (channels), which were formed by the extraction of acid-soluble components, undergo simultaneous transformations (Fig. 6b). As a result, channels up to several tens of angstroms in diameter are formed. These channels are analogous in adsorption properties to the mesopores of ordinary porous silica materials. Moreover, unamalgamated microchannels remained, which are analogous to those in leached soda–silica fiberglass. At low degrees of leaching, the above changes in the texture and composition occurred in surface layers, whereas the structure of the core of fibers remained unaffected. High degrees of leaching resulted in structural transformations of the entire fiber; these transformations are responsible for a considerable loss of strength and even for the degradation of fibers.

ACKNOWLEDGMENTS

We are grateful to L.A. Sergeeva for performing the chemical analysis.

REFERENCES

- Zhdanov, S.P., *Zh. Vses. Khim. o-va im. Mendeleva*, 1989, vol. 34, p. 298.
- Yoo, J.S., Choi-Feng, C., Donobue, J.A., *Appl. Catal.*, 1994, vol. 118, no. 1, p. 87.
- Nicholas, D.M., Shan, Y.T., and Zlochower, I.A., *Ind. Eng. Chem. Prod. Res. Dev.*, 1976, vol. 15, no. 1, p. 29.
- Barelko, V.V., Khalzov, P.I., Zviagin, V.N., and Onischenko, V.Ya., *Proc. II Conf. "Modern Trends in Chemical Kinetics and Catalysis,"* Novosibirsk, 1995, vol. II (1), p. 164.
- Barelko, V.V., Yuranov, I.A., Cherashev, A.V., *et al.*, *Dokl. Ross. Akad. Nauk*, 1998, vol. 361, no. 4, p. 485.
- Kiwi-Minsker, L., Yuranov, I., Holler, V., and Renken, A., *Chem. Eng. Sci.*, 1999, vol. 54, p. 4785.
- Simonova, L.G., Barelko, V.V., Lapina, O.B., *et al.*, *Kinet. Katal.*, 2001, no. 5, p. 693.
- Iler, R.K., *The Chemistry of Silica*, New York: Wiley, 1979.
- Mastikhin, V.M., Lapina, O.B., and Mudrakovskii, I.L., *Yadernyi magnitnyi rezonans v geterogennom katalize* (Nuclear Magnetic Resonance in Heterogeneous Catalysis), Novosibirsk: Nauka, 1992.
- Turner, G.L., Smith, K.A., Kirkpatrick, R.J., and Oldfield, E., *J. Magn. Reson.*, 1986, vol. 67, p. 544.
- Eckert, H., *Prog. NMR Spectrosc.*, 1992, vol. 24, p. 159.
- Engelhardt, G. and Michel, D., *High-Resolution Solid-State NMR of Silicates and Zeolites*, New York: Wiley, 1987.
- Peri, I.B., *J. Phys. Chem.*, 1966, vol. 70, p. 29.
- Benesi, H.A. and Jones, A.C., *J. Phys. Chem.*, 1959, vol. 63, p. 179.